Journal of Photochemistry & Photobiology, B: Biology 171 (2017) 9–19

Contents lists available at ScienceDirect

Journal of Photochemistry & Photobiology, B: Biology

journal homepage: www.elsevier.com/locate/jphotobiol

New isomeric Cu(NO_2-phen)$_2$Br]Br complexes: Crystal structure, Hirschfeld surface, physicochemical, solvatochromism, thermal, computational and DNA-binding analysis

Ismail Warad[a,*], Firas F. Awwadi[b], Malak Daqqa[a], Anas Al Ali[a], Taher S. Ababneh[c], Tareq M.A. AlShboul[c], Taghreed M.A. Jazzazi[d], Fuad Al-Rimawi[e], Taibi Ben Hadda[f], Yahia N. Mabkhot[g]

[a] Department of Chemistry, Science College, An-Najah National University, P.O. Box 7, Nablus, Palestine
[b] Department of Chemistry, The University of Jordan, Amman 11942, Jordan
[c] Department of Chemistry and Chemical Technology, Tafila Technical University, Tafila, Jordan
[d] Department of Chemistry, Yarmouk University, Irbid, Jordan
[e] Chemistry Department, Faculty of Science and Technology, Al-Quds University, P.O. Box 20002, Al-Quds, Palestine
[f] LCM Laboratory, Sciences Faculty, Mohammed Premier University, Oujda 60000, Morocco
[g] Department of Chemistry, College of Science, King Saud University, P.O. Box 2455, Riyadh 1451, Saudi Arabia

ARTICLE INFO

Keywords:
Cu(II) complexes
XRD
Solvatochromism
DFT
DNA-binding

ABSTRACT

Water soluble mono-cationic copper(II) complex of the general formula [Cu(NO_2-phen)$_2$Br]Br, (NO_2-phen = 5-nitro-1.10-phenantholine) was prepared in good yield under ultrasonic irradiation. The desired complex was isolated as a bromide salt and identified by MS, EA, UV–Vis., TG/DTA, FT-IR and XRD. The single-crystal X-ray diffraction and Hirschfield analysis revealed a square pyramidal distorted geometry around the Cu(II) center. The geometry of the [Cu(NO_2-phen)$_2$Br]$^+$ complex was fully optimized with ab-initio methods and (DFT/B3LYP) density functional theory, then structural parameters were compared to the XRD data. The solvatochromism of [Cu(NO_2-phen)$_2$Br]Br complex was investigated in several polar solvents. Absorption and viscosity titration studies concluded that the [Cu(NO_2-phen)$_2$Br]Br complex is a very good CT-DNA binder.

1. Introduction

One of large challenges in medicinal and bioinorganic chemistry is to develop new anticancer active reagents through either lab-synthesis or natural-isolation of such compounds [1–3]. Numerous coordination compounds, such as *cis*-platin complex, have played a critical role as drugs in fighting against certain types of cancer [3–5]. Even with the satisfactory results of *cis*-platin in treating several cancer types, there are still a number of associated disadvantages such as: dose-limiting toxicity, side effects and resistance phenomena [6]. Transition metal ion complexes were engaged to solve such old standing problems [7]. Complexes of copper(I) and (II) showed promising perspectives [8–12] since the metal is an essential trace element in the bodies, and the complexes are water soluble so dose-limitation may be reduced [12].

1,10-Phenanthroline ligand and its derivatives find extensive applications as bidentate chelating ligands in coordination chemistry [13–16]. Many 1,10-phenanthroline and hybrid 1,10-phenanthroline ligands/metal complexes have found interesting medical applications [17].

Copper(II)/1,10-phenanthroline complexes mixed with other ligands received much attention due to their remarkable cytotoxicity which in some cases is more efficient than that of cisplatin [18–20]. Moreover, such complexes are considered one of the most active DNA binding agents, mostly though groove mode causing rapid DNA cleavage [21–25].

Solvatochromism phenomenon in complexes has gained a good awareness in organic and inorganic chemistry because of its implementation in Lewis acids and bases color-indexing [26–28]. Investigating solvatochromism in complexes has yielded a quantitative method to evaluate the role of solvents in understanding the physicochemical features of complexes [29].

Due to the strong Jahn–Teller effect in copper(II) complexes, particularly with coordination number 5, evident solvatochromic was observed [27–29]. Herein, we report the synthesis, solvatochromism, thermal, Hirshfeld surface analysis, computational study and spectroscopic properties of the mono-cation [Cu(NO_2-phen)$_2$Br]Br complex.

* Corresponding author.
E-mail address: warad@najah.edu (I. Warad).

http://dx.doi.org/10.1016/j.jphotobiol.2017.04.017
Received 19 December 2016; Received in revised form 11 March 2017; Accepted 17 April 2017
Available online 25 April 2017
1011-1344/

Table 1
Crystal structure refinement data for [Cu(NO_2-phen)$_2$Br]Br complex.

Empirical formula	$C_{24}H_{17}Br_2CuN_6O_7$	
Formula weight	724.80	
Temperature	293(2) K	
Wavelength	0.71073 Å	
Crystal system	Triclinic	
Space group	P − 1	
Unit cell dimensions	a = 9.9902(6) Å	α = 99.274(5)°
	b = 11.2406(6) Å	β = 105.540(5)°
	c = 13.6643(7) Å	γ = 110.934(5)°
Volume	1323.30(13) Å 3	
Z	2	
Density (calculated)	1.819 Mg/m^3	
Absorption coefficient	3.901 mm^{-1}	
F(000)	716	
Crystal size	0.4 × 0.3 × 0.2 mm^3	
Theta range for data collection	3.23 to 26.30°.	
Index ranges	−9 ≤ h ≤ 12, −14 ≤ k ≤ 13, −17 ≤ l ≤ 16	
Reflections collected	9953	
Independent reflections	5353 [R(int) = 0.0243]	
Completeness to theta = 26.30°	99.8%	
Absorption correction	Semi-empirical from equivalents	
Max. and min. transmission	1.00000 and 0.63506	
Refinement method	Full-matrix least-squares on F^2	
Data/restraints/ parameters	5353/8/395	
Goodness-of-fit on F^2	1.053	
Final R indices [*I* > 2sigma(I)]	R1 = 0.0507, w*R*2 = 0.1192	
R indices (all data)	R1 = 0.0779, w*R*2 = 0.1347	
Largest diff. peak and hole	0.895 and −0.723 e. Å^{-3}	

Table 2
XRD selective bond lengths and angels for [Cu(NO_2-phen)$_2$Br]Br complex.

Bond type		Length(Å)	Angle type			Value(°)
Cu1	Br1	2.416(1)	Br1	Cu1	N1	94.2(1)
Cu1	N1	1.996(5)	Br1	Cu1	N12	120.7(1)
Cu1	N12	2.126(3)	Br1	Cu1	N15	128.0(1)
Cu1	N15	2.106(5)	Br1	Cu1	N26	94.0(1)
Cu1	N26	1.999(5)	N1	Cu1	N12	79.6(2)
N1	C2	1.328(7)	N1	Cu1	N15	95.4(2)
N1	C14	1.355(6)	N1	Cu1	N26	171.8(2)
C2	C3	1.39(1)	N12	Cu1	N15	111.3(2)
C3	C4	1.346(8)	N12	Cu1	N26	95.6(2)
C4	C5	1.405(9)	N15	Cu1	N26	80.1(2)
C5	C6	1.431(7)	Cu1	N1	C2	126.1(4)
C5	C14	1.395(8)	Cu1	N1	C14	115.6(4)
C6	C7	1.329(8)	C2	N1	C14	118.3(5)
C7	C8	1.430(9)	N1	C2	C3	123.0(6)
C7	N29	1.485(7)	C2	C3	C4	119.5(6)
C8	C9	1.416(9)	C3	C4	C5	119.1(6)
C8	C13	1.403(6)	C4	C5	C6	124.0(6)
C9	C10	1.36(1)	C4	C5	C14	118.6(6)
C10	C11	1.373(8)	C6	C5	C14	117.4(5)
C11	N12	1.338(8)	C5	C6	C7	120.8(6)

The crystal structure of the title complex was also investigated.

2. Experimental Section

2.1. Materials

All reagents were of analytical grade and purchased from Sigma–Aldrich and used as received. Elemental analyses were recorded with an Elementar Varrio EL analyzer. The FT-IR spectra (4000–500 cm^{-1}) were obtained with a Perkin–Elmer 621 spectrophotometer. Thermal analyses were carried out in an open air system at a heating rate of 10 °C min^{-1} and a temperature range of 0–1000 °C using TA SDT-Q600 instrument. Electronic spectra were recorded in water at room temperature on Pharmacia LKB-Biochrom 4060 spectrophotometer. Mass spectrometry data were obtained by a Finnigan 711A (8 kV), modified by AMD and reported as mass/charge (*m/z*).

2.2. Synthesis of [Cu(NO_2-phen)$_2$Br]Br Complex

$CuBr_2{\cdot}2H_2O$ (1 mmol) was dissolved in 20 mL of ethanol under

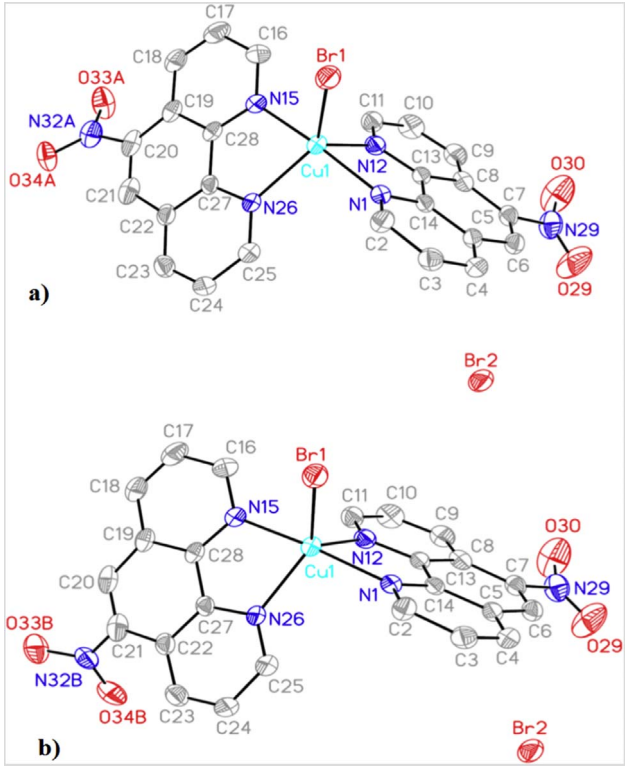

Fig. 1. The ORTEP generated diagram of (a) *cis*-[Cu(NO_2-phen)$_2$Br]Br and (b) *trans*-[Cu(NO_2-phen)$_2$Br]Br isomers. Hydrogen atoms and water molecules are omitted for clarity.

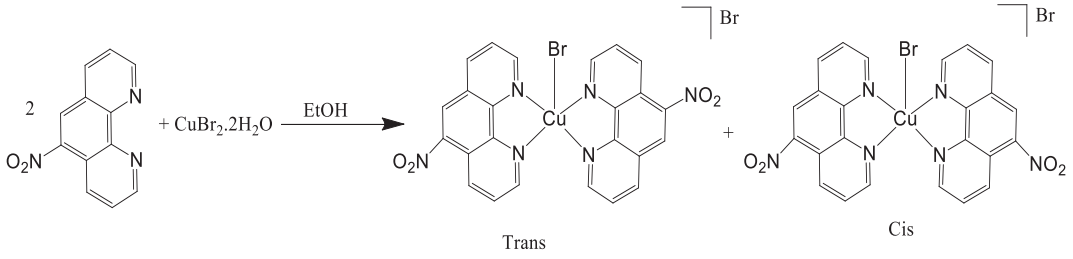

Scheme 1. Synthesis of [Cu(NO_2-phen)$_2$Br]Br complexes.

Table 3
Hydrogen bonds for $[Cu(NO_2\text{-phen})_2Br]^+$ complex [Å and °].

D—H…A	d(D—H)	d(H…A)	d(D…A)	< (DHA)
O(36)—H(36A)…O(37)	1.00	1.85	2.808(11)	160.3
O(37)—H(37B)…Br(2)	0.85	2.42	3.274(4)	177.0
O(37)—H(37A)…Br(2)$^{\#}$1	0.85	2.54	3.339(5)	157.4

Symmetry transformations used to generate equivalent atoms: $^{\#}1 - x + 2, -y + 1, -z$.

ultrasound waves, to which an ethanoic solution (10 mL) of 2.2 mmol of NO_2-phen was added dropwise with stirring for 5 min until a brown precipitate was formed. The product complex was filtrated, washed by dichloromethane to remove excess NO_2-phen ligand and then dried under vacuum. Since the complex is highly soluble in water, crystals suitable for X-ray structural analysis were obtained by slow evaporation of an aqueous solution of the complex, The complex was isolated as a blue powder, with 81% yield, m. p. = 215.0 °C, MS *m/z* 647.90 M^+ due to its mono-cationic nature $[Cu(NO_2\text{-phen})_2Br]^+$ with chemical Formula: $C_{24}H_{20}Br_2CuN_6O_7([Cu(NO_2\text{-phen})_2Br]Br{\cdot}3H_2O)$. Elemental Analysis: Calculated: C, 39.61; H, 2.77; N, 11.55%. Found: C, 39.22; H, 2.74; N, 11.48%. IR: 3402 (ν_{H2O}), 3050 (ν_{C-H} of phen), 1520 ($\nu_{N=C}$), 1330 (ν_{NO2}), 518 (ν_{Cu-N}). UV–Vis. in water: λ_{max} at: 270 nm ($2.8 \times 10^4\ M^{-1}\ L^{-1}$) and 705 nm ($1.8 \times 10^2\ M^{-1}\ L^{-1}$).

2.3. X-ray Single-crystal Data Collection

Several suitable crystals were mounted and the diffraction data were collected at RT using an Oxford Xcalibur diffractometer (Mo Kα radiation, λ = 0.7107 Å). Data was processed using CrysAlisPro software [30]. The structures were solved by direct methods and refined by least-squares method on F2 using the SHELXTL program package [31]. Hydrogen atoms are located on the calculated positions except those

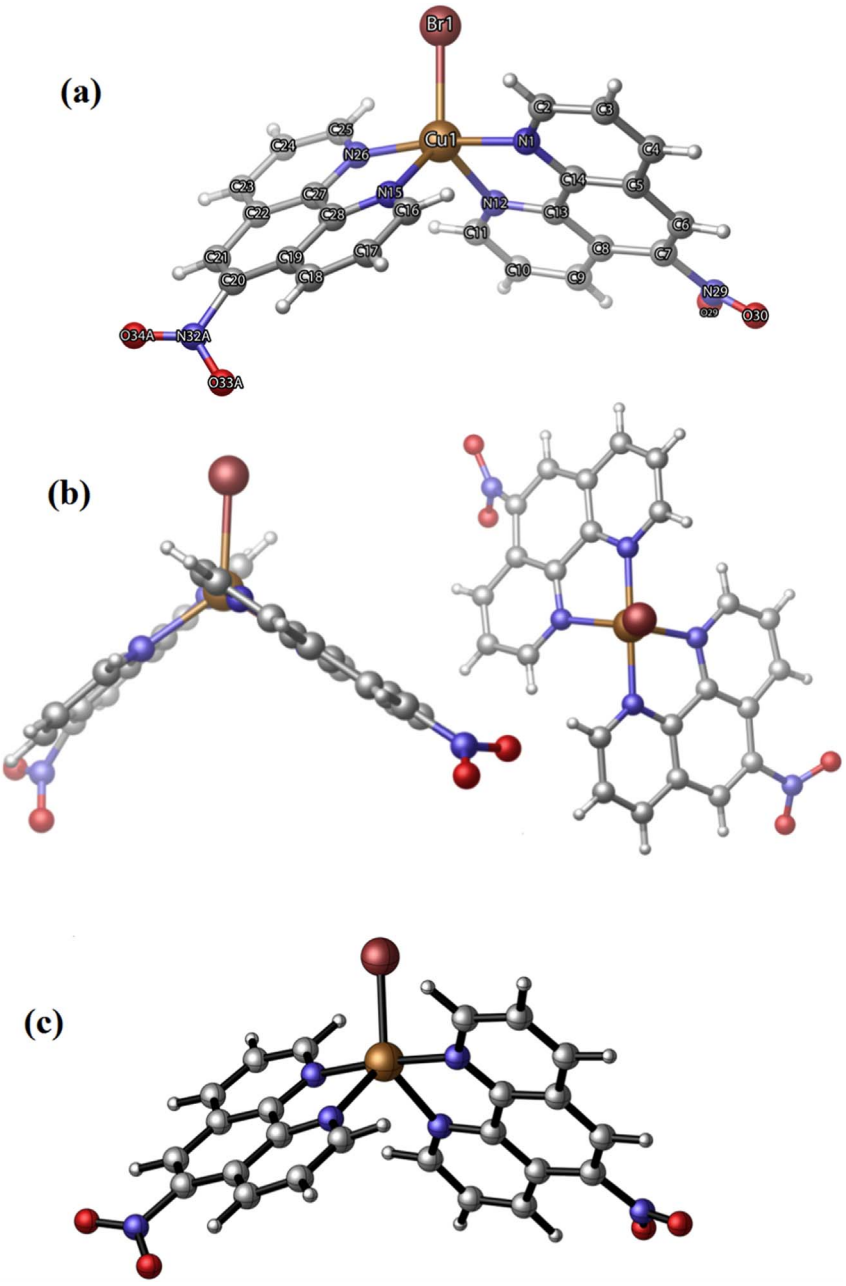

Fig. 2. a) Perspective view of the XRD structure of *cis*-$[Cu(NO_2\text{-phen})_2Br]Br$ showing the atom numbering scheme. b) Side and top views of the X-ray structure. c) The optimized ground state geometry for the copper complex at B3LYP/6-31G (d) level of theory.

Table 4
Selected experimental and calculated bond lengths (pm) and angles (°) of cis/trans-[Cu(NO_2-phen)$_2$Br]Br complex. Calculated values were obtained at the HF/3-21G, HF/6-31G* and B3LYP/6-31G* levels of theory.

Bond (pm)	Exp'l	Calculated HF 3-21G	HF 6-31G*	DFT/B3LYP 6-31G*
Cu1−Br1	241.6	233.2	241.3	240.1
Cu1−N1	199.6	207.0	211.6	201.0
Cu1−N12	212.6	212.4	222.3	216.5
Cu1−N15	210.6	212.4	224.4	216.8
Cu1−N26	199.9	207.0	211.0	201.0
N1−C2	132.8	133.8	132.5	133.3
N1−C14	135.5	135.1	135.2	135.8
C2−H2A	93.0	106.8	107.2	108.5
C2−C3	139.1	140.3	140.6	140.5
C5−C14	139.5	140.7	141.4	141.2
C7−N29	148.5	142.3	144.3	148.2
N29−O30	117.1	134.2	122.6	122.5
N29−O29	119.1	129.9	121.8	122.9
N32A−O33A	122.2	129.9	121.9	123.0
N32A−O34A	122.2	134.2	122.6	122.5
Correlation coefficient (CC)	–	0.97489	0.96605	0.97434
Angle (°)				
Br1−Cu1−N1	94.21	94.98	95.95	92.69
Br1−Cu1−N12	120.71	127.56	131.18	130.31
Br1−Cu1−N15	128.01	127.58	128.24	129.14
Br1−Cu1−N26	94.01	95.00	95.87	92.68
N1−Cu1−N12	79.62	78.65	76.38	79.60
N1−Cu1−N15	95.42	95.27	96.32	97.13
N1−Cu1−N26	171.82	170.02	168.18	174.62
N12−Cu1−N15	111.32	104.86	100.58	100.56
N12−Cu1−N26	95.62	95.12	95.83	96.74
N15−Cu1−N26	80.12	78.66	76.15	79.59
Cu1−N1−C2	126.14	125.53	124.33	125.56
Cu1−N1−C14	115.64	114.27	115.93	115.27
C2−N1−C14	118.35	119.99	119.56	119.13
N1−C2−H2A	118.50	116.53	116.49	116.12
N1−C2−C3	123.06	121.27	122.40	122.44
Correlation Coefficient (CC)	–	0.94912	0.94447	0.95839

attached to water molecules. The hydrogen atoms of two water molecules are located using Fourier difference map, whereas hydrogens atoms of the water molecule (O35) could not be located. Data collection and refinement parameters are given in Table 1.

2.4. Computational Method

The molecular geometry of the title cationic complex was fully optimized without any geometric constraints in the gas phase at the DFT/B3LYP level of theory, which utilizes the three parameter Becke exchange functional, B3 [32], the nonlocal correctional functional of Lee, Yang and Parr (LYP [33]) in conjunction with the polarized 6-31G(d) main set [34]. The starting molecular geometry is extracted from the experimentally determined crystal structure. Additionally, we have employed two ab-initio methods, namely HF/3-21G [35] and HF/6-31G* [36] and reported the geometrical parameters of the optimized complex. All electronic structure calculations were performed using the Spartan 16 package.

2.5. DNA Binding Investigation

2.5.1. Absorption-titration Method

The experimental absorption-titration measurements were carried out in Tris–HCl buffer with 5 mM Tris–HCl, 50 mM NaCl and pH 7.2. 1.0×10^{-5} M Cu(II) concentration was used during the titration process. The CT-DNA concentrations were varied between 0 and 2.0×10^{-2} M by maintaining the volume of the total mixture constant at 10.0 mL. The resulting mixed solutions of Cu(II)/CT-DNA were left standing to equilibrate for 10 min at RT after each trial before subjecting them to absorption measurements at λ_{max} = 270 nm. K_b binding constants were calculated using Eq. (1) [37].

$$[DNA]/(\in_a - \in_f) = [DNA]/(\in_b - \in_f) + 1/K_b(\in_b - \in_f) \quad (1)$$

where [DNA] is the conc. of DNA, εa is the apparent extinction coefficient obtained by calculating A_{obs}/[complex], εf corresponds to the free extinction coefficient of the complex and εb refers to the extinction coefficient of the complex in the bound form. When fitted to the above equation, a straight line with slope of 1 / (εb − εf) and y-intercept of 1/Kb(εb − εf) results. Finally, K_b was determined from the ratio of the slope to intercept.

2.6. Viscosity Measurements

Viscosity experiments were carried out using an Ubbelodhe viscometer at 25.0 (± 0.1) °C. The viscosities, of fixed [DNA] = 5.0×10^{-4} M concentration mixed with complex solutions of different concentrations (0–6.5 × 10^{-5} M), were evaluated. The binding ratio [Cu]/[DNA] was plotted versus $(\eta/\eta^\circ)^{1/3}$ [38], where η° is the pure DNA viscosity and η is the viscosities of DNA in the presence of complex concentrations.

3. Results and Discussion

3.1. Synthesis

Water soluble mono-cationic [Cu(NO_2-phen)$_2$Br]Br complex was prepared in good yield through the direct addition of two equivalents of NO_2-phen ligand to $CuBr_2{\cdot}2H_2O$ dissolved in ethanol under an open RT ultrasonic vibration (Scheme 1). The brown color of the $CuBr_2{\cdot}2H_2O$ ethanolic solution first changed to green when NO_2-phen ligand was added. By the end of the reaction, the product complex was precipitated as a deep-brown powder. The complexes is highly soluble in DMF, DMSO and water, low solubility in ROH and insolubility in chlorinated and hydrocarbon solvents. The complex was found to be stable in solution as well as in the solid phase at ambient conditions.

The complex was isolated as a racemic *cis* and *trans* mixture of mono-cationic bromide salts. Since the NO_2 group at position 5 is relatively far away from the crowded copper center, there is no strict electronic configuration preference, yielding to mixed *cis/trans* isomer structures confirmed only by single crystal X-ray measurements. The complex was also characterized using elemental analysis, thermal, electrochemical, spectral methods and Hirschfield surface analysis.

3.2. Crystal Structure for [Cu(NO_2-phen)$_2$Br]Br Complex

The complex crystallized in Monoclinic system with C2/c space group. All the bond lengths and angles are listed in Table 2.

[Cu(NO_2-phen)$_2$Br]Br complex crystalizes as mixture of two *cis/trans* isomers as seen the ORTEP diagram of the molecule (Fig. 1). The Cu(II) is 5-coordinated center with 1 Br-atom and 4 N-donors of 2 chelating NO_2-phen in a distorted-square pyramidal geometry, three uncoordinated water molecules are present in the crystal lattice. In CuN4Br coordination sphere, Cu1-Br1 bond length of 2.416(1) Å, Cu1−N1, Cu1−N12, Cu1−N15 and Cu−N26 bond lengths 1.996(5), 2.126(3), 2.106(5) and 1.999(5) Å, respectively. The N−Cu−N bond angles range from79.62° to 171.82°. The XRD data is in agreement with the recent reports [1,39,40]. Hydrogen bonding interactions connect water molecules and bromide anions. Hydrogen bond parameters are listed in Table 3.

Bromide counter ion together with the three water molecules don't directly coordinate to the copper(II) center but they stabilize the crystal structure due to many Hydrogen-bonds intermolecular forces formation (Table 3).

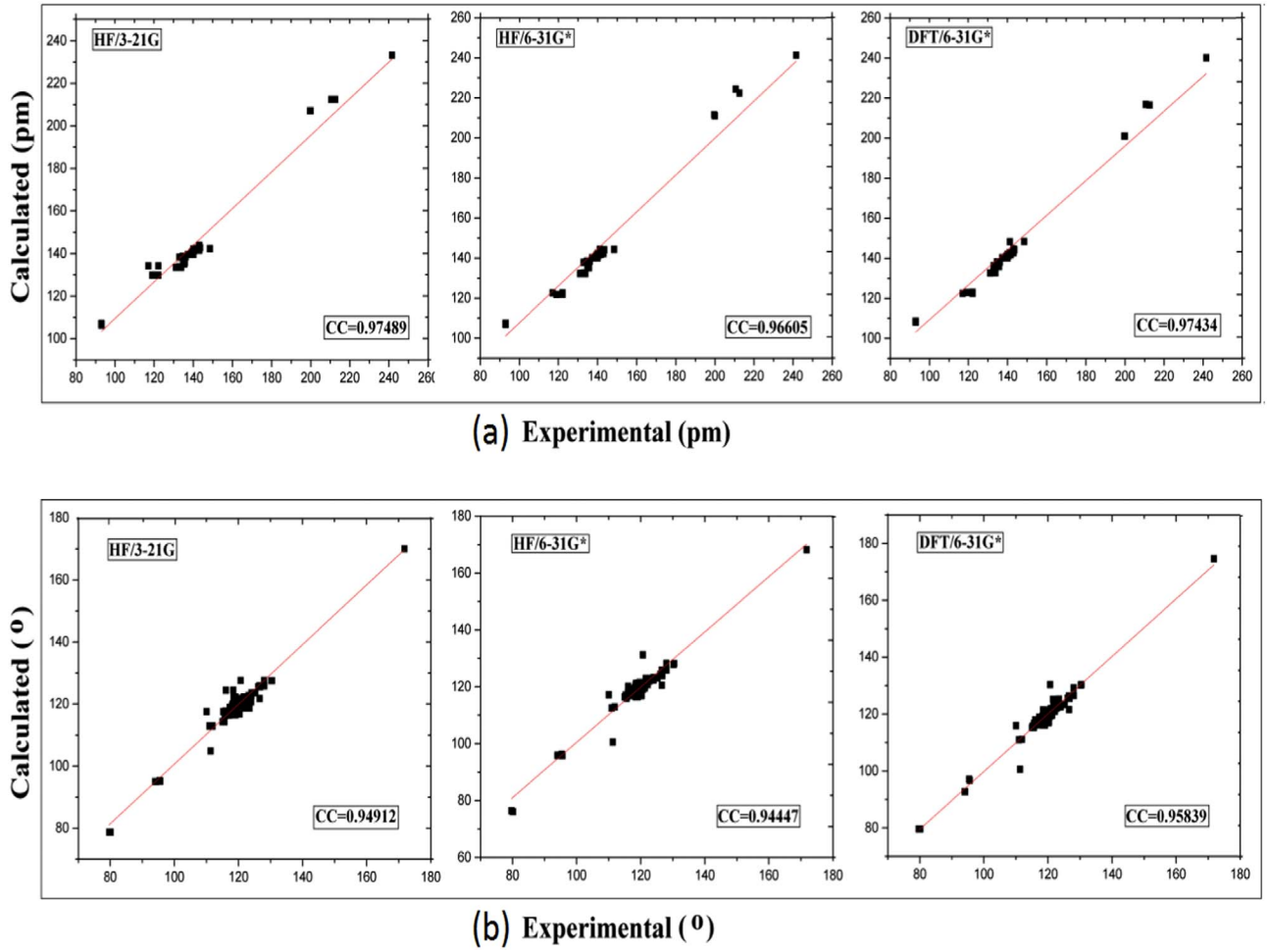

Fig. 3. Graphical correlation between experimentally determined (a) bond lengths (pm) and (b) bond angles (°) versus the calculated values determined by HF/3-21G, HF/6-31G* and B3LYP/6-31G* methods for $[Cu(NO_2\text{-phen})_2Br]Br$ complex.

Table 5
Calculated electronic properties and quantum parameters for $[Cu(NO_2\text{-phen})_2Br]Br$ complex obtained at the B3LYP/6-31G* level of theory.

E (a.u.)	E_{HOMO}(eV)	E_{LUMO}(eV)	ΔE (eV)	I (eV)	A (eV)	X (eV)	η (eV)	σ (eV)	μ (eV)	ω (eV)	D (debye)
− 5766.33347	− 9.06	− 5.91	3.15	9.06	5.91	7.49	1.58	0.635	− 7.49	17.79	2.20

3.3. Computational Study

The compound under investigation is the mono-cationic $[Cu(NO_2\text{-phen})_2Br]^+$ complex. We have examined the complex by carrying out intensive ab-initio and DFT calculations to retrieve the optimized ground state geometry and determine its electronic and quantum parameters. The optimized structure of $[Cu(NO_2\text{-phen})_2Br]^+$ at the B3LYP/6-31G* level of theory is shown in Fig. 2c in combination with views of the x-ray structure of the complex (Fig. 2a and b). The performance of ab-initio methods HF/3-21G [41] and HF/6-31G* [42] along with one of the most commonly used B3LYP/6-31G* [32–36,43,44] model has been tested against selective experimentally determined structural parameters of the complex including bond lengths (pm) and angles (°). The correlation coefficients (CC) for bond lengths (pm) obtained at HF/3-21G, HF/6-31G* and B3LYP/6-31G* are 0.97489, 0.96605 and 0.97434 respectively. Though all tested methods gave high correlation coefficient values for bond lengths, HF/3-21G and B3LYP/6-31G* methods produced the highest correlation coefficients. For bond angles, the calculated correlation coefficients are 0.94912, 0.94447 and 0.95839 for HF/3-21G, HF/6-31G* and B3LYP/6-31G*, respectively. It is apparent that B3LYP/6-31G* method gives the maximum correlation for angles and yields the most satisfactory results for estimating the bond angles of the title compound. Selected calculated and experimental bond lengths (pm) and angles (°) are given in Table 4. Graphical correlations between the experimentally determined bond lengths (pm) and angles (°) versus the calculated values determined by HF/3-21G, HF/6-31G* and B3LYP/6-31G* methods are shown in Fig. 3.

Selected electronic properties and quantum parameters of the title complex were determined and summarized in Table 5. Based on the frontier molecular orbital (FMO) theory, the chemical reactivity is strongly associated with the interaction between the highest occupied molecular orbital (HOMO) and the lowest unoccupied orbital (LUMO) of the reacting species. A molecule with higher value of E_{HOMO} is indicative of its ability and tendency to donate electrons to an accepter molecule with a low E_{LUMO} value. Also, a molecule with a large band gap energy ΔE_{gap} should be less reactive than one having a smaller gap. In the present study, the total energy, the highest occupied molecular orbital (HOMO) energy, the lowest unoccupied molecular orbital (LUMO) energy (Fig. 4), the band gap energy ΔE_{gap}, the ionization

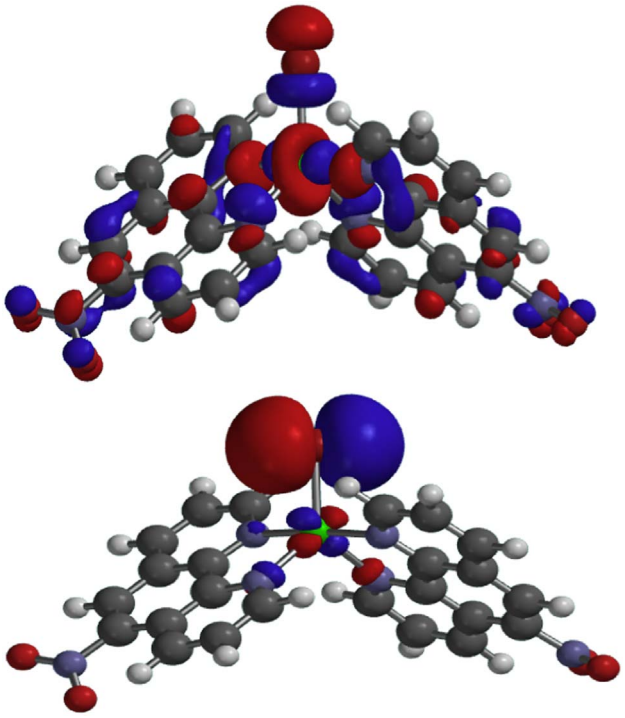

Fig. 4. The HOMO (lower) and LUMO (upper) plots of [Cu(NO_2-phen)$_2$Br]Br complex at the B3LYP/6-31G* level of theory.

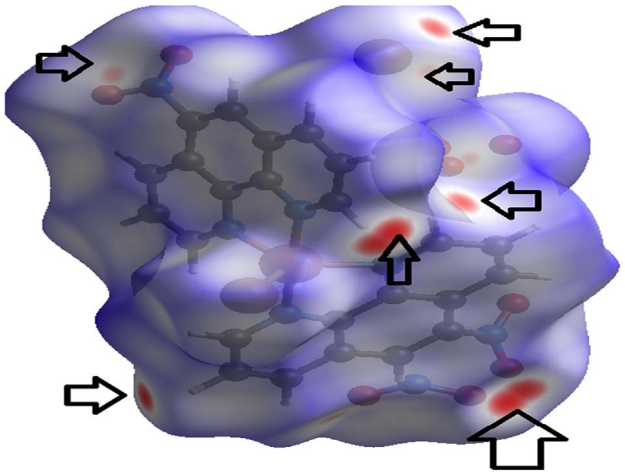

Fig. 5. Hirshfeld surfaces comprising d_{norm} surface plots for [Cu(NO_2-phen)$_2$Br]Br complex.

potential (*I*), the electron affinity (*A*), the absolute electronegativity (*X*), the absolute hardness (η), the softness (σ), the chemical potential (μ), the electrophilicity index (ω) and the dipole moment (*D*) were calculated at the B3LYP/6-31G* level of theory [40–44]. The ionization potential (*I*) and the electron affinity (*A*) can be expressed as $I = -E_{HOMO}$ and $A = -E_{LUMO}$. The absolute electronegativity (*X*), the absolute hardness (η), the softness (σ) and the electrophilicity index (ω) are given by [43]:

$$X = (I + A)/2,\ \eta = (I - A)/2,\ \sigma = 1/\eta \text{ and } \omega = \mu^2/2\eta$$

where μ represents the chemical potential and is given as $\mu = -X$ [44]. The electrophilicity index (ω) is a measure of the electrophilic power of a molecule [41–44]. The hardness (η) and softness (σ) are proportional of the gap between the HOMO and LUMO energies such that hard molecules have a high ΔE_{gap} and soft molecules have a small ΔE_{gap}. Therefore, the hardness is associated with the stability of molecules while the softness is a measure of the extent of chemical reactivity. Calculated reactivity indices of the title compound obtained at the B3LYP/6-31G* method are listed in Table 2.

3.4. Hirschfeld Surface Analysis HSA

HAS is an excellent tool for explaining packing and intermolecular forces in the solved crystal structure [45–50]. It offers a clean picture of intermolecular interactions and molecular shape in a crystalline environment. Surface characteristic like: types of interactions (color coding reveals their strength), the distances from the surface to the nearest interior (di plots) or exterior (de plots) atom.

HSA confirmed the presence of several H-bonds in the crystal structure of the desired complex. N–H….Br with 2.70 Å (see Fig. 5). HSA of the complex revealed several red spots on the surface of the molecule as a result of the H-bond acceptors close to the bromide atoms which may have encouraged and stabilized the crystal formation.

Atom…atom fingerprint contacts with their percentages of HAS contact contribution are illustrated in Fig. 6. [(a) Total, (b) H…all (33.6%), (c) H…0.0 (13.9%), (d) H…H (7.2%), (e) H…Br (7.0%), (f) H…C (4.2%) (h) H…N (1.3%) and (1) H…Cu (0.1%)].

3.5. MS, Elemental Analyses and Conductivity

The mono-cationic nature of the title complex $[Cu(NO_2\text{-phen})_2Br]^+$ was confirmed by MS $[M^+] = 647.90\ m/z$, (theoretical 647.2). The CHN elemental analysis is consistent with the proposed formula $C_{24}H_{20}Br_2CuN_6O_7$, ([Cu(NO_2-phen)$_2$Br]Br·3H_2O) of the complex and the solved XRD structure, because the two isomers in the crystal lattice have the same molecular formula. The combination of water solubility (0.05 g/mL at RT) and conductivity ($220\ \Omega^{-1}\ cm^2\ mol^{-1}$ at RT of 1×10^{-3} M in water) is in agreement with the mono-cationic nature of the complex. This result is also consistent with the XRD data.

3.6. Visible and Ultraviolet Spectra

In virtue of the visible color changes when NO_2-phen ligand was added to the copper-bromide salt in ethanoic solution from brown to green and finally the complex precipitates as brown precipitate, the brown color of the complex changes to light blue when it is re-dissolved in water.

In the UV region, the complex showed two singles at $\sim\lambda_{max} = 270$ and 295 nm (shoulder), which were assigned to π-π electron transfer as seen in Fig. 7a.

In the Vis. region, the complex exhibited one broad absorption band at 705 nm assigned to.

d-d electron transfer as seen in Fig. 7b. No changes were detected on color nor on λ_{max} value when 1×10^{-3} M aqueous solution of the complex was measured after 30 days in an open atmosphere, as in Fig. 7c, which indicates the stability of such complexes.

3.7. Solvatochromism

The solubility of the complexes in polar solvents was limited to the number of solvents which could be investigated by the solvatochromism studies. Water, MeOH, DMF and DMSO were used. The desired mono-cationic complex is solvatochromic in such solvents due to the expected strong Jahn–Teller effect on copper(II) ions (d^9 electron configuration) [26–29,50]. The Vis. spectra of the complex in selected solvents revealed a broad band between 600 and 800 nm. The visible spectral changes of the λ_{max} of the complex with selected solvents are recorded in Fig. 8.

The bathochromic spectrophotometric shifts of the complex is in agreement with the mechanism of solvatochromism behavior in such complexes [29,50], which can be resonated to the direct coordination of the polar solvent molecules onto the vacant sites of the Cu(II) center

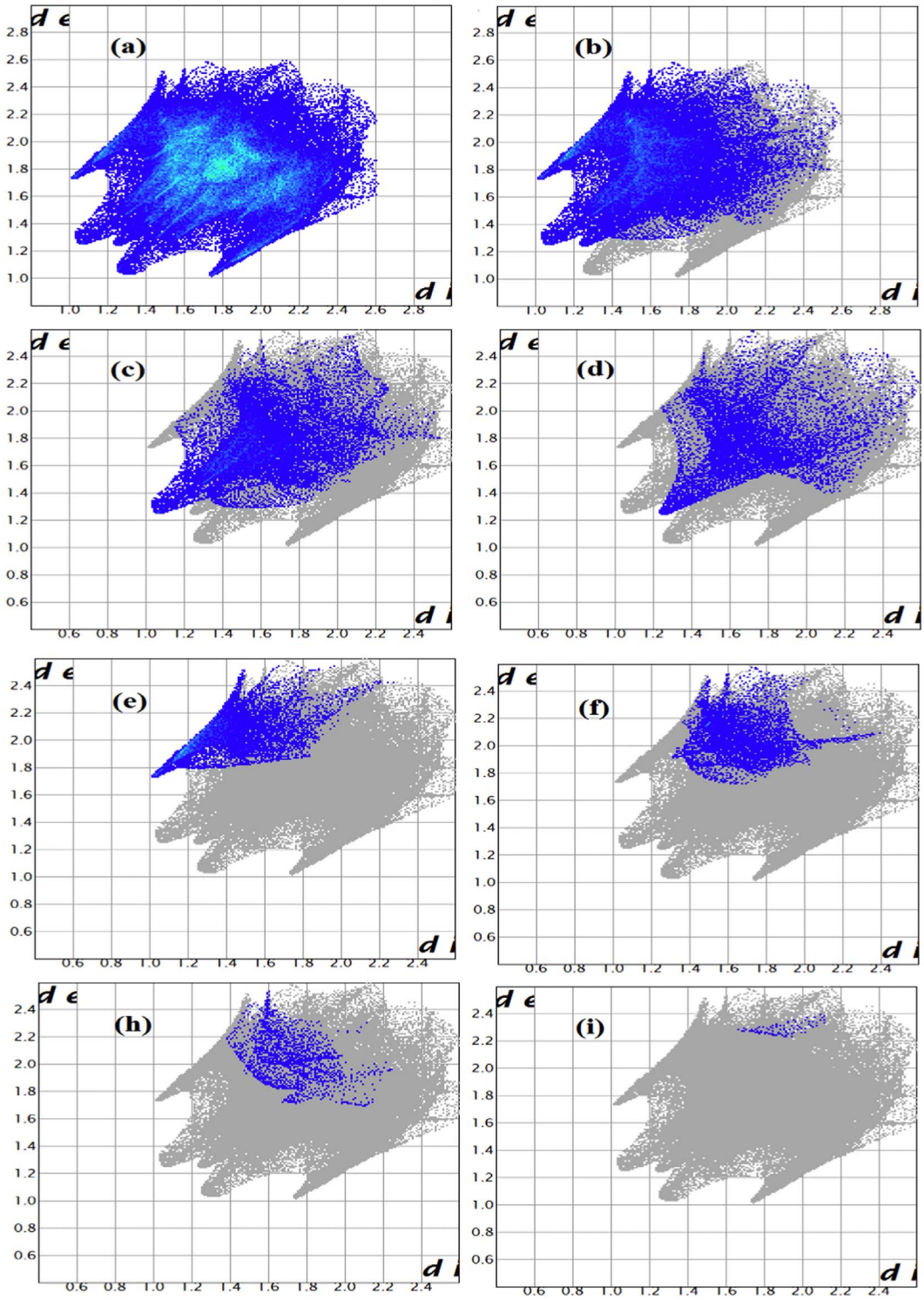

Fig. 6. Fingerprint plots of [Cu(NO_2-phen)$_2$Br]Br complex.

with different strengths.

Accordingly, the λ_{max} values increased linearly with the increasing of the Gutmann's donor number (DN) of the selected solvents. The linear trend of λ_{max} of the complex against DN is presented in Fig. 9.

3.8. FT-IR Spectral Investigation

The complexation reaction was monitored by mid. FT-IR as seen in Fig. 10. The spectra of the 5-NO_2-phen ligand before and after coordination with $CuBr_2$ were recorded in solid state using KBr disk. The main bands at 3410, 3080, 1562 and 1350 cm^{-1} in the free ligand are assigned to the stretching vibrations of several functional groups like: $\nu(H_2O)$, ν(C—H) phen, ν(C═N) and $\nu(NO_2)$, respectively. These bands are shifted to lower wavenumbers upon coordination to Cu(II) center (see experimental part and Fig. 10b). Appearance of a band at 518 cm^{-1} in the complex was due to the $\nu_{(Cu-N)}$ stretching vibration.

3.9. TG/DTG Analyses

The TG/DTG thermal activities of [Cu(NO_2-phen)$_2$Br]Br complex

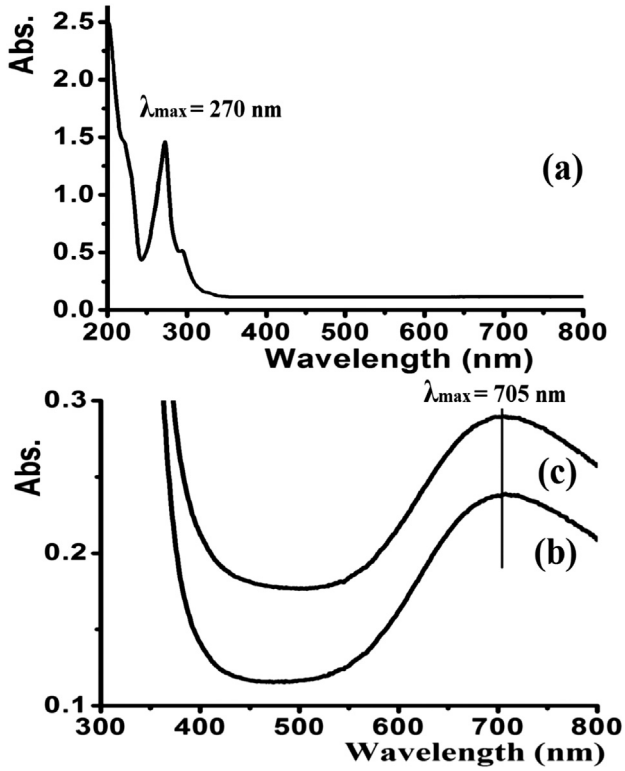

Fig. 7. UV spectrum of $[Cu(NO_2\text{-phen})_2Br]Br$ complex dissolved in water at RT (a) 1×10^{-4} M, Vis. spectra (b) 1×10^{-3} M, fresh dissolved and (c) same solution as in (b) but after 30 days.

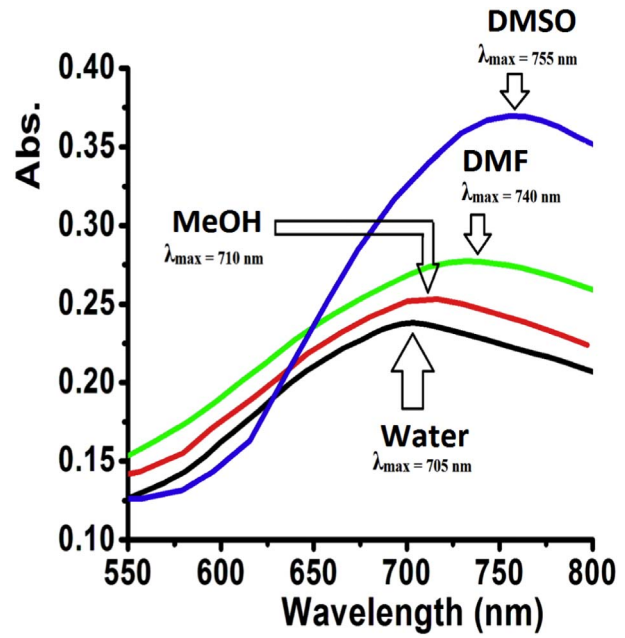

Fig. 8. Absorption spectra of $[Cu(NO_2\text{-phen})_2Br]Br$ complex in dissolvable solvents.

were carried out in an open air system with a heating rate of 10 °C min^{-1} and 0 to 1000 °C range of temperatures. The thermogravimetric data of $[Cu(NO_2\text{-phen})_2Br]Br$ complex showed two consecutive degradation steps; ligands pyrolysis and inorganic residue formation, as seen in Fig. 11.

TG/DTG spectra of the complex were illustrated mainly by three steps of weight loss. The first step was losing of three uncoordinated water molecules at 80–130 °C, losing ~8% of weight (7.5% calculated), which is consistent with the XRD data. The second decomposition was

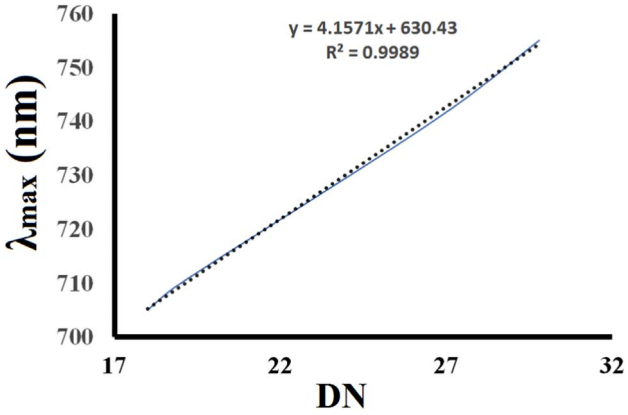

Fig. 9. Dependence of the λ_{max} of $[Cu(NO_2\text{-phen})_2Br]Br$ complex on DN solvent Gutmann's donor numbers.

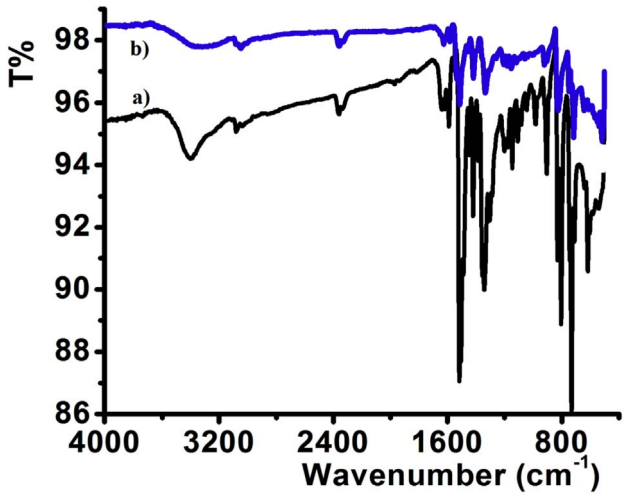

Fig. 10. FT-IR spectra of NO_2-phen free ligand a) and $[Cu(NO_2\text{-phen})_2Br]Br$ complex b).

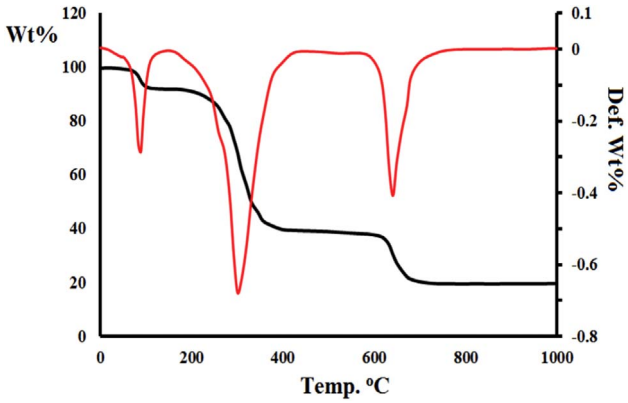

Fig. 11. TG/DTG thermal curves of $[Cu(NO_2\text{-phen})_2Br]Br$ complex.

de-structuring of the two NO_2-phen ligands at 200–400 °C losing ~60% of weight (61.8% calculated) to form the $CuBr_2$ product. The third step which starts from 580 °C and ends at 680 °C may be due to removing of Br ions of $CuBr_2$ and reacting with atmospheric O_2 to form copper oxide as a final product, corresponding to 19.2% weight lost (20% calculated). The final copper oxide product was confirmed by IR.

3.10. DNA Binding Studies

3.10.1. Absorption Spectroscopy

Electronic absorption spectroscopy is considered to be of the most

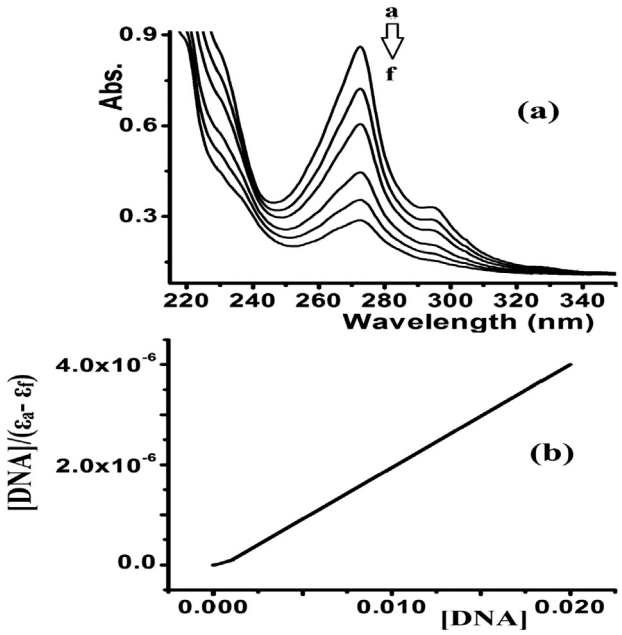

Fig. 12. (a) Electronic spectral titration of $[Cu(NO_2\text{-phen})_2Br]Br$ with CT-DNA at 270 nm in Tris-HCl buffer; [Cu] = 5.0×10^{-5}; [DNA]: *a* 0.0, *b* 5.0×10^{-6}, *c* 1.0×10^{-5}, *d* 1.0×10^{-4}, *e* 1.0×10^{-3}, *f* 2.0×10^{-2} M. The arrow denotes the gradual decrease of $[Cu(NO_2\text{-phen})_2Br]Br$ concentration upon DNA addition. (b) Plot of $[DNA]/(\varepsilon_a - \varepsilon_f)$ vs. [DNA] at λ_{max} = 270 nm to establish the K_b value.

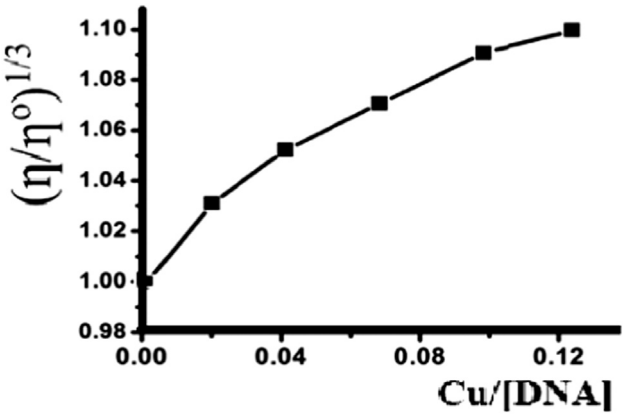

Fig. 13. Effect of increasing amounts of [Cu] on the relative viscosities of DNA at 25.0 (± 0.1) °C, [DNA] = 5.0×10^{-4} M.

important tools to evaluate the binding strength of complexes to DNA [20–26,51–59]. The binding of the desired complex with CT–DNA was evaluated using UV–Vis. spectroscopy to obtain the possible binding modes and to evaluate the K_b constant. DNA binding affinities of phen/Cu(II) complexes were recently reported for several complexes such as: $[Cu(phen)_2Cl_2]\cdot 6H_2O$ (1.89×10^4), $[Cu(phen)(DMF)_2(ClO_4)_2]$ (1.47×10^5), $[Cu(phen)(L\text{-tyr})(H_2O)]ClO_4$ (4.0×10^3), $[Cu\text{-phen}(H_2O)]ClO_4$ (2.44×10^6) and $[Cu(phen)_2$(branched polyethyleneimine)$]Cl_2\cdot 4H_2O$ (5.95×10^5) [51–61].

Previous reports have suggested that materials that bind to DNA through intercalation usually result in bathochromism and hypochromism due to the strong π–π stacking interactions between the aromatic chromophore and DNA base pairs [20–25]. The extent of bathochromism in the UV–Vis. Band supports the strength of intercalative interaction [1].

The electronic Abs. spectra of the complex in the absence and presence of the CT-DNA are shown in Fig. 12. There exists a band at 270 nm, by increasing the concentrations of CT-DNA the absorption band exhibited a significant decrease in absorption with a bathochromic shift of 1–2.2 nm, therefore the complex is suggested to interact with CT-DNA through intercalation mode [1].

Using Eq. (1), a plot was constructed of [DNA]/(εa − εf) vs [DNA] for the titration of DNA with the complex (Fig. 12). K_b value was found to be $1.8 \times 10^4\ M^{-1}$.

3.11. Viscosity Measurements

To further assess the Cu(II)-DNA binding mode, viscosity measurements were utilized in our investigation. A classical intercalative mode suggests that the CT-DNA helix should lengthen as base pairs are separated to accommodate the binding ligand leading to an increase in the molecular weight due to binding the complex, which increases the DNA viscosity [39,52–56]. The effect of $[Cu(NO_2\text{-phen})_2Br]Br$ complex addition on the viscosity of DNA is depicted in Fig. 13.

Increasing of the complex concentration leads to a non-linear increase in the relative viscosity of DNA. The increased degree of viscosity reflects the degree of complex affinity to bind the DNA. The results suggest that the complex binds the DNA double helix through the intercalation mode.

4. Conclusions

Water-soluble mixture of *cis/trans*-$[Cu(NO_2\text{-phen})_2Br]Br$ mono-cationic copper(II) complex were prepared in excellent yield under ultrasonic mode. The mixture of two *cis/trans* isomers in the complex lattice was detected by single-crystal measurement, it is not possible to insulate cis-isomer and trans-isomer all alone. The *cis/trans* mixture complex matrix was fully characterized by elemental analyses, MS, UV–Vis., FT-IR, thermal and XRD analysis. The X-ray single-crystal diffraction along with Hirschfield surface analysis supported the formation of a distorted square pyramidal geometry around the Cu(II) center with several H-bonds. TG recorded a very stable *cis/trans*-complex that decomposed through a three-step process ended by CuO residue. The solvatochromism in several polar solvents suggested that Guttmann's DN parameter is the main contribution in increased λ_{max} of the complex.

The structure of the complex was theoretically studied by ab-initio and DFT methods. The geometry of the complex was fully optimized and the structural characteristics were determined by HF/3-21G and HF/6-31G* ab-initio methods and by DFT at the B3LYP/6-31G* level, and the obtained results are in good agreement with the experimental data. The viscosity and absorption measurements concluded that the desired *cis/trans*-complex is a very good CT-DNA binder. By Cu(II)-DNA absorption titration, K_b was found to be $1.8 \times 10^4\ M^{-1}$ and the binding is through the intercalation mode.

Acknowledgements

The authors extend their sincere appreciation to the Deanship of Scientific Research at King Saud University for its funding this Prolific Research group (PRG-1437-29).

Appendix A. Supplementary data

Supplementary data to this article can be found online at http://dx.doi.org/10.1016/j.jphotobiol.2017.04.017.

References

[1] D. Inci, R. Aydın, O. Vatan, D. Yılmaz, H.M. Genckal, Y. Zorlu, T. Cavas, Binary and ternary new water soluble copper (II) complexes of L-tyrosine and substituted 1, 10-phenanthrolines: effect of substitution on DNA interactions and cytotoxicities, Spectrochim. Acta A: Mol. Spectrosc. 145 (2015) 313–324.

[2] P.R. Reddy, S. Rajeshwar, B. Satyanarayana, Synthesis, characterization of new copper (ii) Schiff base and 1,10 phenanthroline complexes and study of their bioproperties, J. Photochem. Photobiol. B Biol. 160 (2016) 217–224.

[3] F. Arnesano, G. Natile, Mechanistic insight into the cellular uptake and processing of cisplatin 30 years after its approval by FDA, Coord. Chem. Rev. 253 (2009) 2070–2081.
[4] T.W. Hambley, Developing new metal-based therapeutics: challenges and opportunities, Dalton Trans. 43 (2007) 4929–4937.
[5] Y.W. Jung, S.J. Lippard, Direct cellular responses to platinum-induced DNA damage, Chem. Rev. 107 (2007) 1387–1407.
[6] P.C.A. Bruijnincx, P.J. Sadler, New trends for metal complexes with anticancer activity, Curr. Opin. Chem. Biol. 12 (2) (2008) 197–206.
[7] F. Tisato, C. Marzano, M. Porchia, M. Pellei, C. Santini, Copper in diseases and treatments, and copper-based anticancer strategies, Med. Res. Rev. 30 (4) (2010) 708–749.
[8] P. Inamdar, R. Chauhan, J. Abraham, A. Sheela, DNA interaction and cytotoxic activity of copper complex based on tridentate hydrazone derived ligand and nitrogen donor heterocycle, Inorg. Chem. Commun. 67 (2016) 67–71.
[9] L. Jia, J. Xu, X. Zhao, S. Shen, T. Zhou, Z. Xu, T. Zhu, R. Chen, T. Ma, J. Xie, K. Dong, J. Huang, Synthesis, characterization, and antitumor activity of three ternary dinuclear copper (II) complexes with a reduced Schiff base ligand and diimine coligands in vitro and in vivo, J. Inorg. Biochem. 159 (2016) 107–119.
[10] Z. Shokohi-pour, H. Chiniforoshan, A. Abbas, M. Borojeni, B. Notash, A novel Schiff base derived from the gabapentin drug and copper (II) complex: synthesis, characterization, interaction with DNA/protein and cytotoxic activity, J. Photochem. Photobiol. B Biol. 162 (2016) 34–44.
[11] R. Pradhan, M. Banik, D. Cordes, A. Slawin, N. Sah, Synthesis, characterization, X-ray crystallography and DNA binding activities of Co (III) and Cu (II) complexes with a pyrimidine-based Schiff base ligand, Inorg. Chim. Acta 442 (2016) 70–80.
[12] L. Abdel-Rahman, A. Abu-Dief, M. Ismael, M. Mohamed, N. Hashem, Synthesis, structure elucidation, biological screening, molecular modeling and DNA binding of some Cu (II) chelates incorporating imines derived from amino acids, J. Mol. Struct. 1103 (2016) 232–244.
[13] I. Warad, M. Abdoh, N. Shivalingegowda, N.K. Lokanath, R. Salghi, M. Al-Nuri, S. Jodeh, S. Radi, B. Hammouti, Synthesis, spectral, electrochemical, crystal structure studies of two novel di-m-halo-bis[halo(2,9-dimethyl-4,7-diphenyl-1,10-phenanthroline) cadmium(II)] dimer complexes and their thermolysis to nanometal oxides, J. Mol. Struct. 1099 (2015) 323–329.
[14] M. Al-Noaimi, F.F. Awwadi, S.F. Haddad, W.H. Talib, S. Jodeh, S. Radi, T.B. Hadda, M. Abdoh, S. Naveen, N.K. Lokanath, I. Warad, Synthesis, spectral, X-ray single structure, DFT calculations and antimicrobial activities of [Co(II)X2 (dmphen)] (X = Br and SCN), J. Mol. Struct. 1086 (2015) 153–160.
[15] A. Barakat, M. Al-Noaimi, M. Suleiman, A.S. Aldwayyan, B. Hammouti, T.B. Hadda, S.F. Haddad, A. Boshaala, I. Warad, One step synthesis of NiO nanoparticles via solid-state thermal decomposition at low-temperature of novel *Aqua*(2,9-dimethyl-1,10-phenanthroline)$NiCl_2$ complex, Int. J. Mol. Sci. 14 (2013) 23941–23954.
[16] I. Warad, B. Hammouti, T.B. Hadda, A. Boshaala, S.F. Haddad, X-ray single-crystal structure of a novel di-l-chlorobis[chloro(2,9-dimethyl-1,10-phenanthroline)nickel (II)] complex: synthesis, and spectral and thermal studies, Res. Chem. Intermed. 39 (2013) 4011–4020.
[17] D. Wesselinova, M. Neykov, N. Kaloyanov, R. Toshkova, G. Dimitrov, Antitumour activity of novel 1,10-phenanthroline and 5-amino-1,10-phenanthroline derivatives, Eur. J. Med. Chem. 44 (2009) 2720–2723.
[18] Y. Zheng, X. Li, Y. Li, Zh. Wu, C. Yan, Synthesis and structure of new tetracopper(II) complexes bridged by 2-{N′-[2 (dimethylamino)-ethyl]oxamido}benzoate: DNA-binding and anticancer activity, J. Photochem. Photobiol. B Biol. 114 (2012) 27–37.
[19] Z. Tian, Y. Huang, Y. Zhang, L. Song, Y. Qiao, X. Xu, C. Wang, Spectroscopic and molecular modeling methods to study the interaction between naphthalimide-polyamine conjugates and DNA, J. Photochem. Photobiol. B Biol. 158 (2016) 1–15.
[20] V. Uma, M. Kanthimathi, T. Weyhermuller, B. Unnai Nair, Oxidative DNA cleavage mediated by a new copper (II) terpyridine complex: crystal structure and DNA binding studies, J. Inorg. Biochem. 99 (2005) 2299–2307.
[21] S. Mathur, S. Tabassum, Template synthesis of novel carboxamide dinuclear copper (II) complex: spectral characterization and reactivity towards calf-thymus DNA, Biometals 21 (2008) 299–310.
[22] Y.J. Liu, H. Chao, L.F. Tan, Y.X. Yuan, W. Wei, L.N. Ji, Interaction of polypyridyl ruthenium (II) complex containing asymmetric ligand with DNA, J. Inorg. Biochem. 99 (2005) 530–537.
[23] H. Deng, H. Xu, Y. Yang, H. Li, H. Zou, L.H. Qu, L.N. Ji, Synthesis, characterization, DNA-binding and cleavage studies of $[Ru(bpy)_2(actatp)]^{2+}$ and $[Ru(phen)_2(actatp)]^{2+}$(actatp = acenaphthereno [1, 2-b]-1, 4, 8, 9-tetraazariphenylence), J. Inorg. Biochem. 97 (2003) 207–214.
[24] D. Qin, Z. Yang, B. Wang, Spectra and DNA-binding affinities of copper (II), nickel (II) complexes with a novel glycine Schiff base derived from chromone, Spectrochim. Acta, Part A 68 (2007) 912–917.
[25] P.P. Utthra, N. Pravin, N. Raman, Scrutinizing the DNA damaging and antimicrobial abilities of triazole appended metal complexes, J. Photochem. Photobiol. B Biol. 158 (2016) 136–144.
[26] H. Golchoubian, H. Ghorbanpour, E. Rezaee, Dinuclear copper (II) complexes with bridging oximato group: synthesis, crystal structure and solvatochromism property, Inorg. Chim. Acta 442 (2016) 30–36.
[27] S.I. Noro, N. Yanai, S. Kitagawa, T. Akutagawa, T. Nakamura, Binding properties of solvatochromic indicators [Cu (X)(acac)(tmen)](X = PF_6^- and BF_4^-, acac − = acetylacetonate, tmen = *N,N,N′,N′*-tetramethylethylenediamine) in solution and the solid state, Inorg. Chem. 47 (2008) 7360–7365.
[28] R. Horikoshi, Y. Funasako, T. Yajima, T. Mochida, Y. Kobayashi, H. Kageyama, Copper (II) solvatochromic complexes [Cu (acac)(N^N)(ligand)] BPh 4 with various axial ligands. Correlation between coordination geometries and d–d transition energies (acac = acetylacetonato, N^N = 1, 10-phenanthoroline, 2,2′-bipyridyl), Polyhedron 50 (2013) 66–74.
[29] H. Golchoubian, E. Rezaee, G. Bruno, H.A. Rudbari, Synthesis and solvatochromism studies of new mixed-chelate dinuclear copper (II) complexes with different counter ions, Inorg. Chim. Acta 366 (2011) 290–297.
[30] S.K. Wolff, D.J. Grimwood, J.J. McKinnon, D. Jayatilaka, M.A. Spackman, Crystal Explorer 2.1, University of Western Australia, Perth, Australia, 2007.
[31] G.M. Sheldrick, A short history of SHELX, Acta Cryst A64 (2008) 112–122.
[32] A.D. Becke, Density-functional thermochemistry. IV. A new dynamical correlation functional and implications for exact-exchange mixing, J. Chem. Phys. 104 (1996) 1040–1046.
[33] C. Lee, W. Yang, R.G. Parr, Development of the Colic-Salvetti correlation-energy formula into a functional of the electron density, Phys. Rev. B 37 (1988) 785–789.
[34] G.A. Petersson, T.G. Tensfeldt, J.A. Montgomery, A complete basis set model chemistry. III. The complete basis set-quadratic configuration interaction family of methods, J. Chem. Phys. 94 (1991) 6091–6101.
[35] W.J. Hehre, R.F. Stewart, J.A. Pople, Self-consistent molecular-orbital methods. I. Use of gaussian expansions of Slater-type atomic orbitals, J. Chem. Phys. 51 (1969) 2657–2664.
[36] P. Pulay, G. Fogarasi, F. Pang, J.E. Boggs, Systematic ab initio gradient calculation of molecular geometries, force constants, and dipole moment derivatives, J. Am. Chem. Soc. 101 (1979) 2550–2560.
[37] A.M. Pyle, J.P. Rehmann, R. Meshoyrer, C.V. Kumar, N.J. Turro, J.K. Barton, Mixed-ligand complexes of ruthenium (II): factors governing binding to DNA, J. Am. Chem. Soc. 111 (1989) 3051–3058.
[38] M. Ganeshpandian, R. Loganathan, S. Ramakrishnan, A. Riyasdeen, M.A. Akbarsha, M. Palaniandavar, Interaction of mixed ligand copper(II) complexes with CT DNA and BSA: effect of primary ligand hydrophobicity on DNA and protein binding and cleavage and anticancer activities, Polyhedron 52 (2013) 924–938.
[39] A.W. Addision, T.N. Rao, J. Reedijk, J.V. Rijn, G.C. Verschoor, Synthesis, structure, and spectroscopic properties of copper(II) compounds containing nitrogen–sulphur donor ligands; the crystal and molecular structure of aqua[1,7-bis(N-methylbenzimidazol-2′-yl)-2,6-dithiaheptane]copper(II) perchlorate, J. Chem. Soc. Dalton Trans. 7 (1984) 1349–1356.
[40] S. Ramakrishnan, V. Rajendiran, M. Palaniandavar, V.S. Periasamy, B.S. Srinag, H. Krishnamurthy, M.A. Akbarsha, Induction of cell death by ternary copper (II) complexes of l-tyrosine and diimines: role of coligands on DNA binding and cleavage and anticancer activity, Inorg. Chem. 48 (2009) 1309–1322.
[41] K. Fukui, The role of frontier orbitals in chemical reactions (Nobel Lecture), Angew. Chem. Int. Ed. Engl. 21 (1982) 801–809.
[42] A. Lesar, I. Miosev, Density functional study of the corrosion inhibition properties of 1,2,4-triazole and its amino derivative, Chem. Phys. 483 (2009) 198–203.
[43] R.G. Parr, L.V. Szentpaly, S. Liu, Electrophilicity index, J. Am. Chem. Soc. 121 (1999) 1922–1924.
[44] R.G. Parr, R.A. Donnelly, M. Levy, W.E. Palke, Electronegativity: the density functional viewpoint, J. Chem. Phys. 68 (1978) 3801–3807.
[45] M.A. Spackman, D. Jayatilaka, Hirshfeld surface analysis, Cryst. Engg. Comm. 11 (2009) 19–32.
[46] M.A. Spackman, J.J. McKinnon, Fingerprinting intermolecular interactions in molecular crystals, Cryst. Eng. Comm. 4 (2002) 378–392.
[47] C. Tsiamis, M. Themeli, Substituent and solvent effects in the spectra and structure of some mixed-ligand copper (II) chelates containing β-ketoenols, Inorg. Chim. Acta 206 (1993) 105–115.
[48] R. Patel, N. Singh, K. Shukla, J. Nicl'os-Guti'errez, S. Astineiras, V. Vaidyanathan, B. Unni Nair, Characterization and biological activities of two copper(II) complexes with diethylenetriamine and 2,2′-bipyridine or 1,10-phenanthroline as ligands, Spectrochim. Acta, Part A 62 (2005) 261–268.
[49] I. Warad, F. Al-Rimawi, A. Barakat, S. Affouneh, N. Shivalingegowda, N.K. Lokanath, I.M. Abu-Reidah, Synthesis, spectral, thermal, crystal structure, Hirschfeld analysis of [*bis*(triamine)cadimium(II)][cadimum(IV)tetra-bromide] complexes and their thermolysis to CdO nanoparticles, Chem. Cent. J. 10 (2016) 1–11.
[50] F. Abu Saleemh, S. Musameh, A. Sawafta, P. Brandao, C.J. Tavares, S. Ferdov, A. Barakat, A. Al Ali, M. Al-Noaimi, I. Warad, Diethelenetriamine/diamines/copper (II) complexes [Cu(dien)(NN)]Br_2: synthesis, solvatochromism, thermal, electrochemistry, single crystal, Hirshfeld surface analysis and their antibacterial activity, Arab. J. Chem. (2016).
[51] X. Liu, X. Li, Z. Zhang, Y. Dong, P. Liu, C. Zhang, Studies on antibacterial mechanisms of copper complexes with 1, 10-phenanthroline and amino acid on *Escherichia coli*, Biol. Trace Elem. Res. 154 (2013) 150–155.
[52] S. Dey, T. Mukherjee, S. Sarkar, H.S. Evans, P. Chattopadhyay, 5-Nitro-1,10-phenanthroline bis (N, N-dimethylformamide-K′ O)-bis (perchlorato) copper (II): synthesis, structural characterization, and DNA-binding study, Transit. Met. Chem. 36 (2011) 631–636.
[53] Z. Yang, Y. Wang, G. Yang, Copper (II) complex of 1, 10-phenanthroline and L-tyrosine with DNA oxidative cleavage activity in the gallic acid, Biometals 24 (2011) 737–745.
[54] P.R. Reddy, P. Manjula, Synthesis, characterization, and DNA-binding studies of mononuclear copper (II)–phenanthroline–tyrosine complex, Chem. Biodivers. 6 (2009) 71–78.
[55] M.N. Patel, D.S. Gandhi, P.A. Parmar, Synthesis, biological aspects and SOD mimic activity of square pyramidal copper (II) complexes with the 3rd generation quinolone drug sparfloxacin and phenanthroline derivatives, Inorg. Chem. Commun. 14 (2011) 128–132.
[56] A. Prisecaru, V. McKee, O. Howe, G. Rochford, M. McCann, J. Colleran, M. Pour, N. Barron, N. Gathergood, A. Kellett, Regulating bioactivity of Cu2 + bis-1, 10-phenanthroline artificial metallonucleases with sterically functionalized pendant

carboxylates, J. Med. Chem. 56 (2012) 8599–8615.
[57] T.K. Goswami, S. Gadadhar, A.A. Karande, A.R. Chakravarty, Photocytotoxic ferrocene-appended (L-tyrosine) copper (II) complexes of phenanthroline bases, Polyhedron 52 (2013) 1287–1298.
[58] F. Xue, C.-Z. Xie, Y.-W. Zhang, Z. Qiao, X. Qiao, J.-Y. Xu, S.-P. Yan, Two new dicopper (II) complexes with oxamido-bridged ligand: synthesis, crystal structures, DNA binding/cleavage and BSA binding activity, J. Inorg. Biochem. 115 (2012) 78–86.
[59] T. Pivetta, F. Isaia, G. Verani, C. Cannas, L. Serra, C. Castellano, F. Demartin, F. Pilla, M. Manca, A. Pani, Mixed-1, 10-phenanthroline–Cu (II) complexes: synthesis, cytotoxic activity versus hematological and solid tumor cells and complex formation equilibria with glutathione, J. Inorg. Biochem. 114 (2012) 28–37.
[60] M. Al-Noaimi, M.I. Choudhar, F.F. Awwadi, W.H. Talib, T. Ben Hadda, S. Yousuf, A. Sawafta, I. Warad, Characterization and biological activities of two copper (II) complexes with dipropylenetriamine and diamine as ligands, Spectrochim. Acta, Part A 127 (2014) 225–230.
[61] M. Mohamadi, S.Y. Ebrahimipour, J. Castro, M. Torkzadeh-Mahani, Synthesis, characterization, crystal structure, DNA and BSA binding, molecular docking and in vitro anticancer activities of a mononuclear dioxido-uranium (VI) complex derived from a tridentate ONO aroylhydrazone, J. Photochem. Photobiol. B Biol. 158 (2016) 219–227.